

Multiple Target Tracking Using a Narrowband RF Sensor Array

Chris Kreucher

Integrity Applications Incorporated
Ann Arbor, MI 48108
ckreucher@integrity-apps.com

Braham Himed

RF Technology Branch
AFRL/RYMD WPAFB, OH
Braham.Himed@wpafb.af.mil

Abstract—¹ This paper describes a method for detecting and tracking multiple moving targets using a multistatic narrowband radar sensor array. We show that the appropriate model for the sensor array measurements is non-linear and the statistics are non-Gaussian. We use this model in conjunction with a Bayesian estimation algorithm which constructs a probability density on the number of targets and their states. The density is approximated using a novel hybrid discrete grid/particle filter. We evaluate the performance on a set of experimental data from a 6-channel array to detect and track two targets that cross, make sharp turns, and move nearly cross-radially to some pairs for a significant portion of the collect.

I. INTRODUCTION

This paper describes an approach for using measurements from a multistatic narrowband (NB) Radio Frequency (RF) sensor array to detect and track targets. The main contribution is the description of a non-Gaussian non-linear statistical signal processing approach that is robust in the presence of multiple targets, crossing targets, and targets performing difficult-to-model behavior like sharp turns. The performance is evaluated using data collected from a 6-channel multistatic array with just 2% fractional bandwidth.

A NB sensor array has several benefits over a conventional wideband sensor. First, commercial use has eroded the available spectrum often leaving only a small portion for other uses [1]. Furthermore, a NB sensor array is inexpensive due to simple electronics and antennas, and has low power requirements. But perhaps most importantly, an sensor array provides geometric diversity useful for detection and tracking.

Target detection and tracking using a multistatic sensor array has received increased attention in the literature, including [2]–[6]. In our application, we use measurements from a multistatic narrowband RF array, where each bistatic pair (channel) generates a pixelated range/Doppler surface. We model this return surface with a non-linear and non-Gaussian statistical model. We then use these measurements and the statistical model in a Bayes-optimal estimation engine to construct a probability density on the number of targets and their states. What results is a robust multitarget estimation procedure that can detect and track targets through complex maneuvers.

The paper proceeds as follows. Section II describes the sensor array and a statistical model for its measurements. Next,

Section III describes a Bayesian method of state estimation which exploits measurements from this model. We highlight our unique numerical method which uses a hybrid discrete grid/particle filter representation of the high-dimensionality posterior. Finally, in Section IV, we illustrate the approach with an experiment that includes two crossing targets walking an irregular path.

II. STATISTICAL SENSOR MODEL

In our N -element sensor array, each sensor transmits a NB RF signal, which is reflected off targets and clutter and received at each sensor. This process repeats N times, with each sensor serving as transmitter, giving N^2 channels. Fourier processing on the received data generates a bistatic range/range surface.

The bistatic range/range-rate surfaces are related to the xy state of the target non-linearly, and are corrupted by noise. Let $z_{ij}(t, r)$ denote the envelope-detected (non-thresholded) measurement in the $(i, j)^{th}$ bistatic range/range-rate cell from transmitter t and receiver r . Each cell corresponds to a particular bistatic range and range-rate from that sensor pair. The number of cells N_r and $N_{\dot{r}}$ and the resolutions δr and $\delta \dot{r}$ are determined by the radar parameters. For example, the bistatic range resolution is given by $\delta r = c/BW$, where c is the speed of light and BW is the radar bandwidth. Similarly, the bistatic range-rate resolution is given by $\delta \dot{r} = c/f_c T$, where f_c is the radar center frequency, and T is the coherent pulse interval. The collection of measurements is the matrix

$$z(t, r) = \begin{pmatrix} z_{11} & \cdots & z_{1N_D} \\ \vdots & \ddots & \vdots \\ z_{N_r, 1} & \cdots & z_{N_r N_D} \end{pmatrix}, \quad (1)$$

where N_d and N_r are the number of range and range-rate bins.

Let the vector $x = [x, \dot{x}, y, \dot{y}]$ describe the true position and velocity of a target. The statistics of the observation $z_{ij}(t, r)$ in cell (i, j) from transmitter t and receiver r depend on a number of physical factors, including the proximity of cell (i, j) to the true bistatic range and bistatic range-rate of the target; the target impulse response; where the target is in the illumination and receive beams; and whether the receiver is saturated with direct-path energy from the transmitter. Given the small size of the surveillance region and wide sensor beamwidth, we model the pixel proximity and impulse response function only.

¹This work was supported by The Air Force Research Laboratory, contracts FA8650-09-M-1549 and FA8650-10-C-1718.

We model the statistics in each cell as Rayleigh. Let $p(z_{ij}(t, r); x)$ denote the probability of receiving z in bistatic range/range-rate cell (i, j) given a transmitter at t , a receiver at r , and a target at x . The statistical model is then

$$p(z_{ij}(t, r)|x) = 2 \frac{z_{ij}(t, r)}{\lambda_{ij}^2(x; t, r)} \exp\left(-\frac{z_{ij}(t, r)^2}{\lambda_{ij}^2(x; t, r)}\right), \quad (2)$$

where $\lambda_{ij}(x; t, r)$ is a pixel-dependent Rayleigh mode which accounts for the physical factors by specifying the energy expected in cell (i, j) . We assume that, conditioned on the target state, noise is independent across pixels and channels and write the joint multi-channel likelihood as

$$p(z|x) = \prod_{t,r} \prod_{ij} 2 \frac{z_{ij}(t, r)}{\lambda_{ij}^2(x; t, r)} \exp\left(-\frac{z_{ij}^2(t, r)}{\lambda_{ij}^2(x; t, r)}\right), \quad (3)$$

where the notation $\prod_{t,r}$ is to be interpreted as specifying a product over all transmit/receive pairs, and z is the collection of all measurements from all transmit/receive pairs.

In order to capture the proximity of cell (i, j) to the true range/range-rate values, let

$$\Delta_{ij}(x; t, r) = \begin{pmatrix} h_{ij}^R - R(x; t, r) \\ h_{ij}^{\dot{R}} - \dot{R}(x; t, r) \end{pmatrix}, \quad (4)$$

where $R(x; t, r)$ is the function that maps the target state x to a bistatic range and $\dot{R}(x; t, r)$ is the function that maps the target state x to a bistatic range-rate, i.e.,

$$R(x; t, r) = \sqrt{(x - r_x)^2 + (y - r_y)^2} + \sqrt{(x - t_x)^2 + (y - t_y)^2}$$

and

$$\dot{R}(x; t, r) = \frac{(x - r_x)\dot{x} + (y - r_y)\dot{y}}{\sqrt{(x - r_x)^2 + (y - r_y)^2}} + \frac{(x - t_x)\dot{x} + (y - t_y)\dot{y}}{\sqrt{(x - t_x)^2 + (y - t_y)^2}}$$

and h_{ij}^R and $h_{ij}^{\dot{R}}$ are functions that map (i, j) to bistatic range and bistatic range-rate, respectively. Here, they quantize the true range and range-rate to the sensor resolution, and wrap around at the range and range-rate ambiguities. With these definitions, our statistical model is then fully specified as

$$\lambda_{ij}(x; t, r) = \lambda_B + (\lambda_T - \lambda_B) \exp(-\Delta_{ij}^T A \Delta_{ij}),$$

where λ_B and λ_T are the background and target mode parameters, and the matrix A specifies the range and range-rate extent of the main lobe and the cross coupling.

III. BAYESIAN ESTIMATION APPROACH

We use the sensor array measurements to estimate the number of targets in the region and their states (positions and velocities) over time. Our approach is to recursively estimate the joint multi-target probability density at time k ,

$$p(x_1^k, x_2^k, \dots, x_T^k, T^k | Z^k), \quad (5)$$

where T^k is the number of targets, their states are x_1, \dots, x_T and Z^k represents the collection of all measurements up to and including the time k from all channels. For shorthand, we write this as $p(X^k, T^k | Z^k)$, where the cardinality of X^k is implied by T^k . The density can be expressed as the product of the target number density $p(T^k | Z^k)$ and the target state density $p(X^k | T^k, Z^k)$, i.e.,

$$p(X^k, T^k | Z^k) = p(T^k | Z^k)p(X^k | T^k, Z^k). \quad (6)$$

The target state density is updated according to the rules of Bayesian mathematics. It is predicted forward in time via

$$p(X^k | T^k, Z^{k-1}) = \sum_{T^{k-1}} \int p(X^k, T^k | X^{k-1}, T^{k-1}) \times p(X^{k-1}, T^{k-1} | Z^{k-1}) dX^{k-1}, \quad (7)$$

where the integral is to be interpreted as performing the T^{k-1} integrations required. The density is updated with a new measurement at time k called z^k according to Bayes rule as

$$p(X^k | T^k, Z^k) \propto p(z^k | X^k, T^k)p(X^k | T^k, Z^{k-1}). \quad (8)$$

Association is implicit and done by computing the likelihood of the measurement given joint target state, in principle for all multiple target states. No explicit measurement-to-target association is performed. The probability mass function on target number $p(T^k | Z^k)$ is updated analogously.

This density is non-Gaussian due to the measurements, which precludes conventional methods (e.g., Kalman or extended Kalman filters). It is also high dimensional due to the joint multi-target state space. Our implementation employs a unique hybrid discrete grid/particle filter.

In a discrete grid approach, a region is divided into a fixed, evenly spaced, $N_x \times N_{\dot{x}} \times N_y \times N_{\dot{y}}$ grid. The primary benefit is to generate probability estimates over a defined region of state space, only assuming the density is zero outside of the grid boundaries. Conversely, the main deficiencies are that the discrete grid approach spends computational effort updating grid cells with near-zero probability, and that the estimation error is dictated by the grid cell size.

In a particle approach, a density is approximated using particles x_p^k and weights w_p^k as $p(x^k | Z^k) \approx \sum_{p=1}^{N_p} w_p^k \delta(x^k - x_p^k)$. This adaptive grid approach chooses tie-points x_p^k online via importance sampling. For certain classes of problems, the particle approach provides excellent estimation performance at a fraction of the cost of a discrete grid. Thus, its main strengths are that computational effort is only used in areas of high probability, and the grid adaptively changes. The main deficiency is this sparse sampling approach is ill-suited to represent very broad densities, such as a density which has uniform uncertainty over a large spatial region.

For these reasons, we use a hybrid approach which inherits the best features of the two. The density is first approximated on a discrete grid. Once the target present probability exceeds a threshold, a target is present and has been well localized.

At this point, the density is transitioned to a particle approximation by sampling from the discrete grid. This allows sustained detection and tracking with greater precision than the discrete grid. The discrete grid continues to be updated with new measurements to detect the second, third, etc. targets.

An additional feature of our approach is that when multiple targets are in close proximity, a joint multi-target particle filter is formed and the targets are updated jointly [9]. This means that the likelihood of the measurements received is evaluated using the joint target state at once, rather than as a product of the likelihoods from the single target state. This feature ameliorates the track coalescence problem (i.e., two crossing targets both jump on to the single strongest target) since the joint measurement likelihood is lower when there are unexplained measurements. It also reduces the effect a reflection that originated from target *a* can have on the estimate of target *b* by explicitly modeling the fact that both targets are in the scene and that multiple reflections are expected.

This scheme makes several approximations to allow efficient computation. The effects are studied elsewhere [7] and summarized here. First, using a single-target detection surface means that multiple closely spaced targets will take longer to be detected than with the exact Bayesian method. Furthermore, the spatial and velocity resolution of the detection grid limits the precision of the target state estimate relative to the exact Bayesian method. The particle filter for transitioned targets addresses this fact. Next, treating detected targets with a particle filter introduces the diversity problems. In practice, this problem is dealt with by using an efficient importance density [8]. Finally, treating targets as well separated and then thresholding to decide when they should be treated jointly introduces the potential that targets that are close together are inappropriately treated as well separated. In practice this problem is not important since the threshold for close can be set very loosely with no significant harm in treating targets jointly that could have been treated singly.

IV. EXPERIMENTAL RESULTS

The method is illustrated using a four-antenna sensor array while two moving targets walked in a region. We used a commercially available AKELA AVMU500A radar and inexpensive omni-directional antennas. An image of the placement of the antennas in the array is shown in Fig. 1. The layout of the region and target path is shown in Fig. 2.

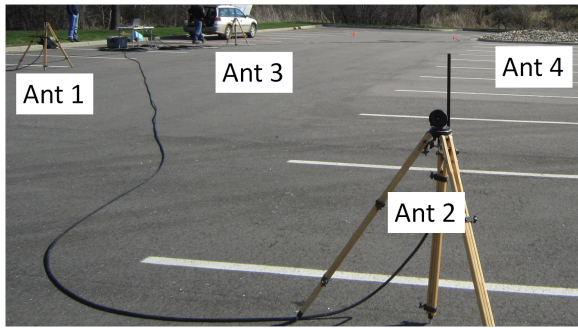


Figure 1. The Four Antennas as Placed for this Experiment.

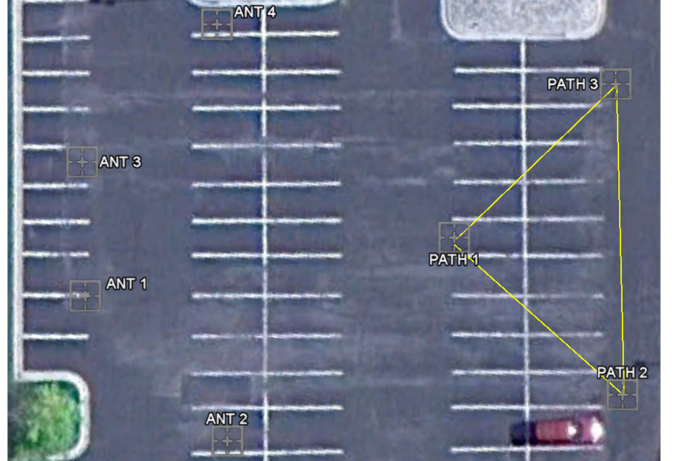


Figure 2. A view of the scene from overhead with the antenna positions (at left) and path points (at right) marked. Image (c) 2011 Google.

We collected data from the six unique bistatic pairs (i.e., $\text{Tx1} \rightarrow \text{Rx2}$, $\text{Tx1} \rightarrow \text{Rx3}$, etc.) with $f_c = 2.43\text{GHz}$, and $BW = 60\text{MHz}$ (about 2% fractional bandwidth).

In this stepped-chirp single-radar multiple-antenna system, the collection proceeded as follows: First, Antenna 1 transmitted a short pulse at the lowest frequency (2.4 GHz). The returns was received by Antenna 2. Next, Antenna 1 transmitted a short pulse at the second-lowest frequency (2.043 GHz), which was received by Antenna 2, and so on, until the highest frequency (2.46 GHz) was completed. The process was repeated between Antenna 1 and Antenna 3 and then between Antenna 1 and Antenna 4, and so on. The individual sweep pulses proceeded at 45 kHz, but the overall rate was dictated by the number of sweep pulses per pair (here chosen to be 40), the number of bistatic pairs (here there were six pairs), and the switching times. In this experiment, the actual complete-cycle pulse-repetition frequency (measured between the time the first sweep pulse was transmitted between Antenna 1 and Antenna 2 and then repeated again) was about 100Hz.

We selected a 0.5s CPI. Combining this choice with the radar parameters above, the resulting data had 5m bistatic range resolution, 0.3m/s bistatic range-rate resolution, 200m unambiguous range and 20m/s unambiguous range rate. These parameters are encoded into h^R and $h^{\dot{R}}$. Empirically, the impulse response has $\sigma_R = 2.5\text{m}$ and $\sigma_{\dot{R}} = 0.6\text{m/s}$. These parameters are encoded into the matrix A . Calibration collects show $\lambda_B = 2500$ and $\lambda_T = 10000$ are good estimates of the background and target modes.

The approach described in Section III was executed using a $25\text{m} \times 16\text{m/s} \times 25\text{m} \times 16\text{m/s}$ detection grid discretized to $51 \times 21 \times 51 \times 21$ cells and particle filters with 1000 particles. Two targets walked the triangle path outlined in Fig. 2. One target walked clockwise and the other counter-clockwise, which resulted in three periods where the targets crossed paths during the 120s collection time. One of the targets carried a handheld GPS unit which approximately truthed the path the targets walked (although at some points the targets deviated from the nominal path by as much as 1m). Fig. 3 shows the performance of the estimation algorithm by indicating the

position estimates for each target for the entire collection. It also gives covariance ellipses for the target state near the crossing points.

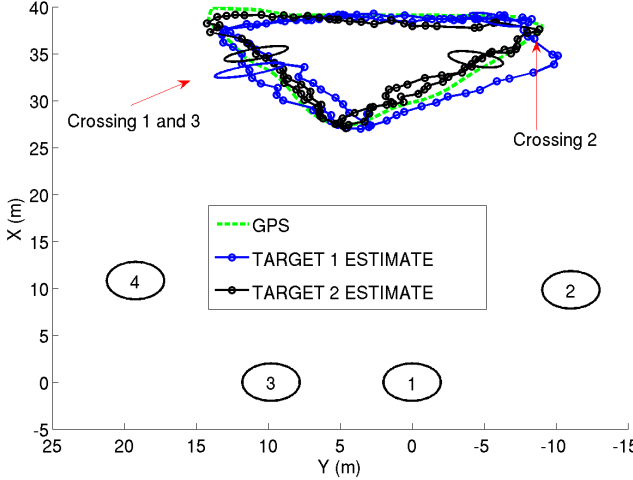


Figure 3. Tracker Output, showing the antenna locations, two target state estimates, and GPS truth of the path.

As mentioned above, the targets cross three times during the collection. Figs. 4 and 5 are images taken from a video camera showing the targets before, during, and after the crossing. The tracker point estimate and uncertainty about target position is projected onto the images for reference. As can be seen from the figures, the method holds track identity through the crossing.

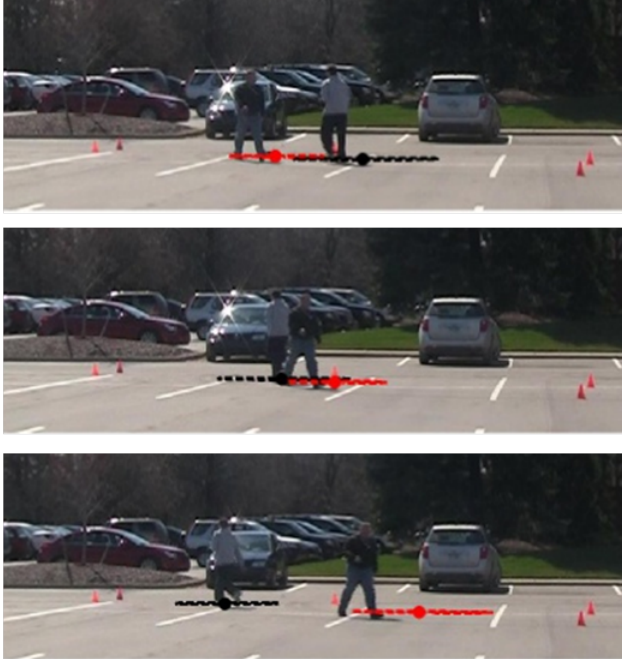


Figure 4. A sequence of images showing the first crossing. The images show the targets immediately before, during, and after the cross. The tracker estimated position and uncertainty of the target states is drawn in for reference.

V. CONCLUSION

This paper has described a method for using a multi-channel radar array to detect and track multiple moving targets. The algorithm combines a non-linear non-Gaussian statistical sensor model on array measurements with a Bayesian estimation scheme. The performance of the method was illustrated with an experiment using a 6-channel array to track two targets that cross, make sharp turns, and move nearly cross-radially to some pairs for a significant portion of the collect.

ACKNOWLEDGMENT

The authors would like to thank Mike Brennan, Ben Shapo, Ben Hart, Joe Burns, and Jim Ebling for assistance in acquiring test data.

REFERENCES

- [1] B. Himed, H. Bascom, J. Clancy and M. Wicks, Tomography of Moving Targets, *Proceedings of SPIE*, 4540, pp. 608-619, 2001.
- [2] K. Bell and R. Pitre, MAP-PF 3D position tracking using multiple sensor array, *Sensor Array and Multichannel Signal Processing Workshop*, 2008.
- [3] Y. Lili, S. Razul, L. Zhiping, S. Chong-Meng, Target tracking in mixed LOS/NLOS environments based on individual TOA measurement detection, *Sensor Array and Multichannel Signal Processing Workshop*, 2010.
- [4] M. Tobias and A. Lanterman, Probability hypothesis density-based multi-target tracking with bistatic range and Doppler observations, *Radar, Sonar and Navigation*, IEE Proceedings, vol. 152, no. 3, pp. 195-205.
- [5] T. Lang and G. Hayes, Exploitation of bistatic Doppler measurements in multistatic tracking, *IEEE Conference on Information Fusion*, 2007.
- [6] B. La Cour, Bayesian Multistatic Tracking with Doppler-Sensitive Waveforms, *OCEANS 2007*, pp. 1-6, June 2007.
- [7] C. Kreucher and B. Shapo, Multitarget Detection and Tracking using Multi-sensor Passive Acoustic Data, *IEEE Journal of Oceanic Engineering*, vol. 36, no. 2, pp. 205-218, April 2011.
- [8] M. Morelade and C. Kreucher and K. Kastella, A Bayesian Approach to Multiple Target Detection and Tracking, *IEEE Transactions on Signal Processing*, vo. 55, no. 5, pp. 1589-1604, May 2007.
- [9] C. Kreucher and K. Kastella and A. Hero, Multitarget Tracking using the Joint Multitarget Probability Density, *IEEE Transactions on Aerospace and Electronic Systems*, vo. 41, no. 4, pp. 1396-1414, October 2005.

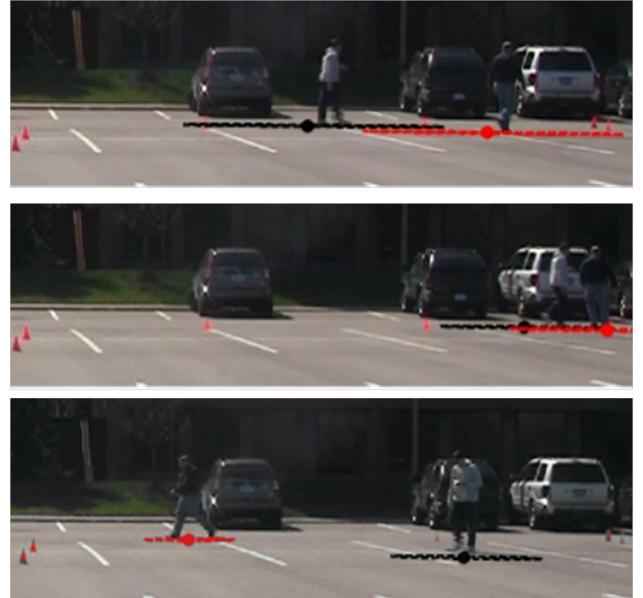


Figure 5. A sequence of images showing the second crossing. The images show the targets immediately before, during, and after the cross. The tracker estimated position and uncertainty of the target states is drawn in for reference.